Small Subsidence of the 660-km Discontinuity Beneath Japan Probed By ScS Reverberations

Mamoru Kato, Mika Misawa, and Hitoshi Kawakatsu

Earthquake Research Institute, University of Tokyo, Tokyo, Japan

Abstract. We investigate layering structure in the mantle beneath Japan using ScS reverberation waveforms of two recent large deep events in the northwest Pacific. We estimate regional variation of the elastic and anelastic structure of the mantle as well as properties of the major velocity discontinuities by modeling broadband seismograms recorded at two dense networks, J-Array and FREESIA. The 660-km discontinuity is the deepest in the region where the stagnant subducting slab in the transition zone is tomographically imaged, but the subsidence is of ~10 km, much smaller than previous estimates with SS precursors. No significant elevation is detected for the 410-km discontinuity.

Introduction

A family of ScS phases (ScS, $sScS$, and their multiples) and reflections from internal discontinuities from regional deep earthquakes are useful tools to investigate regional variation of the mantle layering, powerfulness of which is proven by a series of studies by *Revenaugh and Jordan* [1989, 1991]. Most internally reflected phases have a family of dynamic analogs [*Revenaugh and Jordan*, 1989], and multiplicity of their sampling would provide the path-averaged characteristics of the structure. The transition zone discontinuities are often hypothesized as signatures of phase transitions of the olivine minerals. Clapeyron slopes for the postulated reactions are of opposite signs at the 410-km and 660-km discontinuities (hereafter abbreviated to *410* and *660*, respectively) [*Bina and Helffrich*, 1994], and their topography is expected to be anticorrelated, the deflections be the largest in subduction zones.

We study layering of the mantle beneath Japan by taking advantage of two dense regional broadband networks in Japan, FREESIA and J-Array. Some tomographic studies have imaged a stagnant slab lying in the transition zone beneath Japan [e.g., *Fukao et al.*, 2000], but how the slab interacts with the transition zone discontinuities has not been fully understood yet. By modeling observed broadband seismograms, we investigate regional variation of depths and brightness of the dis-

continuities as well as of elastic and anelastic properties of the mantle. Our results indicate that the stagnant slab apparently controls the topography of *660*, but the subsidence is smaller than previously reported.

Data and Method

Two recent events in the northwest Pacific provide opportunity to demonstrate capability of the Japanese broadband arrays; 1998/08/20, Bonin Islands (Harvard CMT: 28.99 N, 139.47 E, 425.5 km, Mw 7.1), and 1999/04/08, China-Russia Border (43.66 N, 130.47 E, 575.4 km, Mw 7.1) events (Fig. 1). Velocity records are rotated in the horizontal plane after sensor responses are corrected, and the transverse components are filtered between 5 and 30 mHz. To further improve the signal-to-noise ratio, traces are stacked together in two groups for each event after normalized by their respective amplitude of ScS (Fig. 2). Differences of the epicentral distances are less than 2 degrees in each group, and moveouts of the reverberation phases are negligibly small.

Synthetic seismograms are calculated with our ray theory-based code that is optimized for ScS reverberations. All rays that are reflected less than twice at the mantle discontinuities (zero-th to second order phases) are included in the synthetics (Fig. 3). Crustal reverberations are separately treated to include higher order reverberations. Accuracy of our synthetics is tested against Direct Solution Method (DSM) synthetics [*Geller and Takeuchi*, 1995]. Ray theory has the advantage of computational efficiency, and is suited for grid-search optimization; synthetic seismograms are cross-correlated with data seismograms using a 3300 seconds time window (from ScS to $sScS_4$), and goodness of models is evaluated with resultant cross-correlation coefficients. Models are independently derived in four regions. The source is assumed as a delta function in time and space. Epicentral locations are fixed at CMT values. Source depths, d_s, and relative radiation ratios between the upgoing and downgoing S waves (ScS_n and $sScS_n$ phases), e_s, are estimated as model parameters.

Our reference model is AK135 [*Kennett et al.*, 1995]. Velocities are independently perturbed in the upper and lower mantle (ΔV_{UM} and ΔV_{LM}). Lower mantle velocities are increased slightly ($+0.5 \sim +0.8$ %) to match observed whole mantle ScS travel times (τ_{ScS}) initially. Discontinuities are assumed to be sharp, and are de-
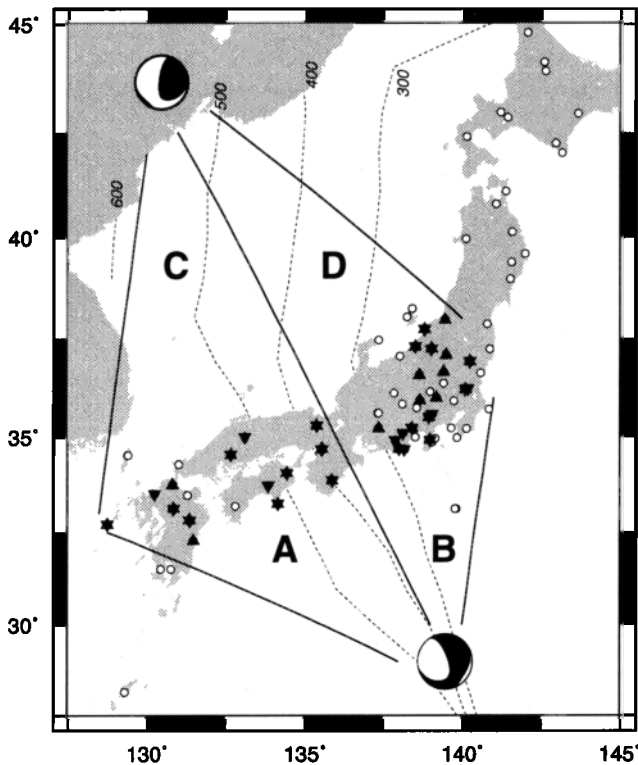
Figure 1. Map of study area. Triangles and inverse triangles are stations used for events 1 and 2, respectively (hexagrams indicate stations used for both events). Open circles indicate unused stations. Harvard CMTs are plotted at the epicentral locations. Dotted lines are isodepth contours for deep seismicity (300-600 km).

Uncertainty bounds are estimated in the grid search. According to χ^2 statistics, if all model parameters are uncorrelated, the variance becomes $N/(N - m)$ times as large as that for the best model when the model is exactly 1σ away from it, where N and m indicate degrees of freedom (corrected for bandpass filtering), and number of model parameters, respectively. Correlation coefficients are related to variance reductions, and we can then estimate ranges of model parameters which correspond to 1σ (Fig. 4). Some parameters are obviously correlated so that our estimates should provide conservative bounds.
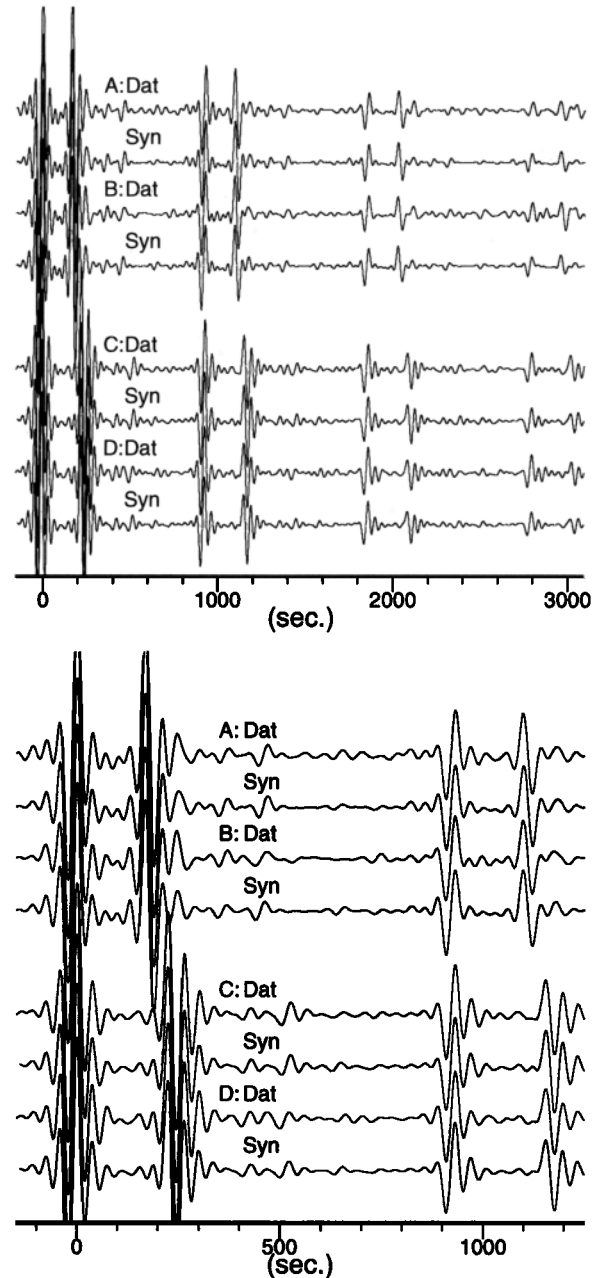

Figure 2. Stacked and synthetic seismograms calculated for the best fitting models (Table 1). Origin of time axis is at ScS phase. (top) The entire waveform. Four pairs of large amplitude phases are $(ScS_n, sScS_n)$, where n=1-4. (bottom) Close up of the waveforms between ScS_1 and $sScS_2$.

scribed by depths (D_{Moho}, D_{410}, and D_{660}), and reflection coefficients for vertical incidence for SH wave (R_{Moho}, R_{410}, and R_{660}). The latter are corrected for non-vertical incidence in waveform synthesis. Attenuation is assumed to be frequency independent. A two-layer model is adopted for the mantle, Q for the upper (Q_{UM}) and lower (Q_{LM}) mantle being separately parameterized; relative amplitudes of top- and bottom-side reflections from 660 could be used to distinguish them. The small data size, however, limits our ability to resolve Qs. Q_{crust} is fixed at 600.

The grid-search optimization is conducted in several steps to model small internally reflected phases as well as large parent phases. Parameters that strongly control zero-th order phases (ScS_n and $sScS_n$), such as source and Moho parameters and Qs, are examined first. Velocity perturbations are estimated next, together with d_s, D_{660}, Qs; these control the waveforms of reflected phases at 660. Search for D_{410}, R_{410}, and R_{660} concludes the optimization process. Experiments with DSM synthetics assure our resolving capability with the current source-receiver geometry. Once the best fitting models are derived with the stacked data, individual traces are similarly processed for the discontinuity depths, using Qs and ΔVs estimated with the corresponding stacks.
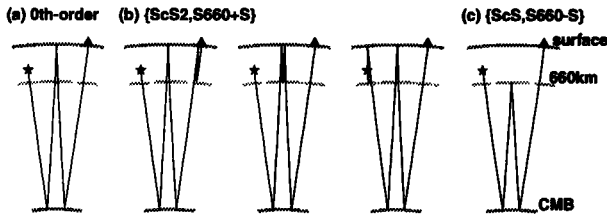
Figure 3. Examples for ray paths of ScS reverberations phases. a) Zero-th order phase ScS_2. b) First order topside reflected phase at 660, $\{ScS_2, S660_+S\}$. This phase has three dynamic analogs, which have the same ray parameter and travel time, but are reflected at different locations. c) First order underside reflected phase at 660, $\{ScS_2, S660_-S\}$. We follow the notation of *Revenaugh and Jordan* [1989].

Results

Table 1 summarizes our models for four regions. Synthetic seismograms calculated for these models explain the observed waveforms well (Fig. 2). We hereafter focus on D_{660} and Q, and other findings will be discussed in our next report.

Arithmetic averages of estimates in four regions of Q_{ScS} (185) and τ_{ScS} (935.9 sec) agree well with estimates by *Revenaugh and Jordan* [1991] for this region (corridor 10), 183, and 935.8 sec, respectively. The depth of 660 in Region B, which covers the Izu-Japan path, also agrees their result (657 vs. 656 km; note the reference models are different). Our results indicate lateral variation of the structure within their single corridor. Lateral variation of Q or of the crustal thickness may potentially bias estimates of other model parameters, and cautions must be taken in interpreting their estimates in heterogeneous corridors.

Q_{ScS} in the Japan Sea ($\sim$220) is higher than that in the Pacific side ($\sim$165), and this difference is well constrained by the large amplitude zero-th order phases.

Our estimates of Q_{UM} are slightly larger than those by *Flanagan and Wiens* [1994], but in Japan Sea are consistent with those by *Nakanishi* [1980]. Almost 2-to-1 variation of Q_{LM} is also observed with an independent, small data set [*Misawa*, 2000]. A heterogeneous boundary layer at the base of the lower mantle could potentially explain such variation of Q_{LM}. However, since amplitudes of seismic phases are controlled by its reciprocal, $1/Q$, resolving its lateral variation is in principle difficult in high Q regions. Our estimates could also be slightly biased by the simplicity of the model, and further study with additional data is needed before we interpret such sharp lateral variation of Q. $R_{660}s$ are smaller than PREM (7.9%) prediction but are consistent with AK135 (6.9%). $R_{410}s$ are slightly smaller than AK135 predictions (4.8%).

Discussions

The largest subsidence occurs in Region A where the stagnant slab is tomographically imaged [e.g., *Fukao et al.*, 2000]. The amount of (excess) subsidence is approximately 10 km, more than a factor of 2 less than estimates from SS precursors, $\sim$20-30 km [*Flanagan and Shearer*, 1998; *Gu et al.*, 1999]. Despite dense sampling by SS precursors in this region, their results could be suffered from the use of the geometrical optics [*Neele et al.*, 1997; *Chaljub and Tarantora*, 1997]. This discrepancy between ScS and SS studies could be resolved if SS precursor data are re-interpreted with less restricting approximations. High frequency studies have implicated larger depression of 660 in Region B [*Collier and Helffrich*, 1997; *Castle and Creager*, 1998]. Distribution of their observations apparently has two peaks, at $\sim$670 and $\sim$700 km, which might implicate fine structure of this discontinuity, the latter be related to garnet minerals [*Niu and Kawakatsu*, 1996; *Vacher et al.*, 1998]. Small subsidence of 660 beneath the northern Philip-
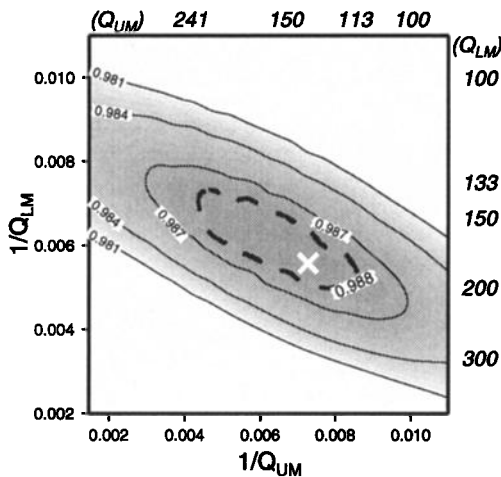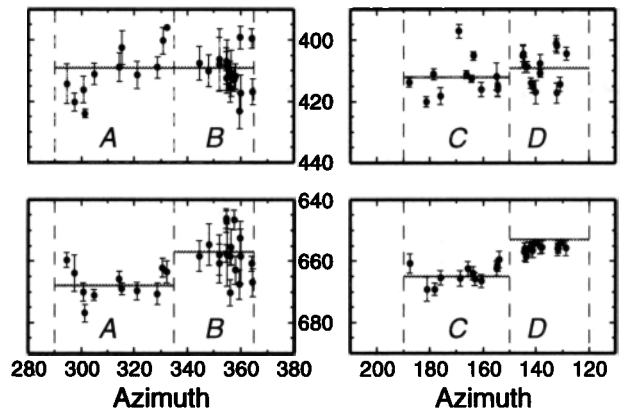

Figure 4. Results of grid search for Qs in Region A, as indicated by contours of correlation coefficients. The cross indicates the best model, and the dashed-line contour indicates the range for 1σ.

Figure 5. Estimated depths of the 410 and 660 from individual traces, as functions of the azimuth from the source, measured clockwise from north. Horizontal gray lines indicate the estimates from the stacked waveforms. Errors for individual data points are estimated with the similar method for the stacked data.

Table 1. Best fitting models

Regions	A	B	C	D
d_s	434	435	571	570
	(432, 435)	(433, 437)	(569, 573)	(567, 572)
e_s	0.93	0.97	0.86	0.86
	(0.85, 0.99)	(0.80, 1.15)	(0.79, 0.90)	(0.79, 0.90)
D_{Moho}	17	10	28	28
	(12, 19)	(-[a] 19)	(26, 30)	(26, 30)
R_{Moho}	0.15	0.11	0.15	0.18
	(0.11, 0.19)	(-[a] 0.20)	(0.13, 0.18)	(0.16, 0.21)
ΔV_{UM}	0.0	0.4	-0.6	-0.6
	(-0.2, 0.4)	(0.0, 0.8)	(-0.8, -0.2)	(-0.8, -0.4)
ΔV_{LM}	0.8	0.6	0.7	0.6
	(0.5, 1.0)	(0.4, 0.8)	(0.5, 0.9)	(0.4, 0.8)
Q_{UM}	139	130	122	94
	(113, 241)	(87, 256)	(87, 184)	(78, 139)
Q_{LM}	176	176	375	375
	(133, 200)	(130, 258)	(240, 850)	(239, 850)
Q_{ScS}[b]	165	161	237	205
D_{660}	668	657	665	654
	±1	± 1	± 1	± 1
R_{660}	0.069	0.059	0.070	0.065
	± 0.003	± 0.003	± 0.003	± 0.003
D_{410}	409	409	412	409
	± 2	± 2	± 1	± 1
R_{410}	0.034	0.044	0.045	0.044
	± 0.003	± 0.003	± 0.003	± 0.003

[a]Lower bound is limited by zero.
[b]Arithmetrically derived from Q_{UM} and Q_{LM}.

pine Sea is suggested from regional triplicated P phases [*Tajima and Grand*, 1998]. Lack of *410* elevation implies that this slab related heterogeneity is localized near *660*.

Despite large width of the Fresnel volume (~several 100 km), estimates with the individual traces have apparently continuous west dipping trends both in Pacific and in Japan Sea (Fig. 5), though the scatters are large. Larger scatters in Region B might reflect lower signal-to-noise ratio due to disturbance of the wavefield by the subducting Pacific Plate. From the current path coverage, we cannot distinguish whether the subsidence of *660* in Regions A and C shares the same origin. Assuming the equilibrium, if this subsidence is attributed solely to the thermal anomaly with the stagnant slab, subsidence of 10-km implies that the temperature variation in the lower transition zone is approximately 150 °C. Alternatively, *660* is a chemical boundary, and is gravitationally depressed by the stagnant slab.

References

Bina, C.R., and G. Helffrich, Phase transition Clapeyron slopes and transition zone seismic discontinuity topography, *J. Geophys. Res., 99*, 15,853-15,860, 1994.

Castle, J. C., and K.C. Creager, Topography of the 660-km seismic discontinuity beneath Izu-Bonin: implication for tectonic history and slab deformation, *J. Geophys. Res., 103*, 12,511-12,527, 1998.

Chaljub, E., and A. Tarantora, Sensitivity of SS precursors to topography on the upper-mantle 660-km discontinuity, *Geophys. Res. Lett., 24*, 2613-2616, 1997.

Collier, J.D., and G.R. Helffrich, Topography of the "410" and "660" km discontinuities in the Izu-Bonin subduction zone, *Geophys. Res. Lett., 24*, 1535-1538, 1997.

Flanagan, M.P., and P.M. Shearer, Global mapping of topography on transition zone velocity discontinuities by stacking SS precursors, *J. Geophys. Res., 103*, 2673-2692, 1998.

Flanagan, M.P., and D.A. Wiens, Radial upper mantle attenuation structure of inactive back arc basins from differential shear wave measurements, *J. Geophys. Res., 99*, 15,469-15,485, 1994.

Fukao, Y., S. Widiyantoro, and M. Obayashi, Stagnant slabs in Bullen's transition region, *Rev. Geophys.*, submitted, 2000.

Geller, R.J., and N. Takeuchi, A new method for computing highly accurate DSM synthetic seismograms, *Geophys. J. Int., 123*, 449-470, 1995.

Gu, Y., A.M. Dziewonski, and C.B. Agee, Global decorrelation of the topography of transition zone discontinuities, *Earth Planet. Sci. Lett., 157*, 57-67, 1999.

Kennett, B.L.N., E.R. Engdahl, and R. Buland, Constraints on seismic velocities in the Earth from traveltimes, *Geophys. J. Int., 122*, 108-124, 1995.

Misawa, M., ScS Reflection Seismology with J-Array data, M. Sc. thesis, 65 pp., Dept. Earth and Planetary Physics, Univ. Tokyo, Mar. 2000 (in Japanese).

Nakanishi, I., Attenuation of shear waves in the upper mantle beneath the Sea of Japan, *J. Phys. Earth, 28*, 261-271, 1980.

Neele, F., H. de Regt, and J. VanDecar, Gross errors in upper mantle discontinuity topography from PdP and SdS data, *Geophys. J. Int., 129*, 194-204, 1997.

Niu, F., and H. Kawakatsu, Complex structure of mantle discontinuities at the tip of the subducting slab beneath Northeast China; a preliminary investigation of broadband receiver functions. *J. Phys. Earth, 44*, 701-711, 1996.

Revenaugh, J. and T.H. Jordan, A study of mantle layering beneath the western Pacific, *J. Geophys. Res., 94*, 5787-5813, 1989.

Revenaugh, J. and T.H. Jordan, Mantle layering from ScS reverberations, 3. The upper mantle, *J. Geophys. Res., 96*, 19,781-19,810, 1991.

Tajima, F., and S.P. Grand, Variation of transition zone high-velocity anomalies and depression of 660 km discontinuity associated with subduction zones from the southern Kuriles to Izu-Bonin and Ryukyu, *J. Geophys. Res., 103*, 15,015-15,036, 1998.

Vacher, P., A. Mocquet, and C. Sotin, Computation of seismic discontinuity profiles from mineral physics: The importance of the non-olivine components for explaining the 660 km depth discontinuity, *Phys. Earth Planet. Inter., 106*, 275-298, 1998.

Wessel, P., and W.H.F. Smith, New version of the Generic Mapping Tools released, *Eos Trans. AGU, 76*, 329, 1995.

M. Kato, H. Kawakatsu, and M. Misawa, Earthquake Research Institute, University of Tokyo, Bunkyo, Tokyo, 113-0032, Japan. (e-mail: mkato@eri.u-tokyo.ac.jp)